Optimization of Hydrogen Injection Flow Rate for Hydrogen Internal Combustion Engines Based on IQGA

Ping Guo*, Jianlun Xu, Minghao Wang

School of Mechanical Engineering, North China University of Water Resources and Power, Zhengzhou 450045, China

Abstract: The density of hydrogen is extremely low, and during fuel supply, hydrogen gas will rapidly expand from the hydrogen injection port into the intake duct, leading to air supply blockage. To eliminate intake blockage in hydrogen fueled internal combustion engines and improve their overall performance. This article investigates the effects of different hydrogen injection rates (hydrogen injection pressure and nozzle diameter) on the performance of hydrogen internal combustion engines at low speeds, based on an improved quantum genetic algorithm (IQGA) and a combination weighting method. The results show that compared with the standard quantum genetic algorithm (QGA), IQGA has faster convergence speed and higher convergence accuracy. By using IQGA to optimize the nozzle diameter and hydrogen injection pressure, it can be concluded that when 3mm and 1.5bar are selected for hydrogen internal combustion engines, intake blockage is less likely to occur; Changing the nozzle diameter and hydrogen injection pressure separately has a significant impact on the flow state of the mixed gas in the inlet duct, and the nozzle diameter has a more significant effect on the inlet blockage than the hydrogen injection pressure. The coupling effect of the two is reflected in the impact of the hydrogen injection mass flow rate on the flow state of the mixed gas in the inlet duct. There is a strict linear relationship between the hydrogen injection mass flow rate and the maximum return flow rate. When the hydrogen injection mass flow rate is not higher than 2.29kg/h, before the inlet valve is closed, No intake back flow occurs; through the combination weighting method, it can be concluded that the comprehensive performance of hydrogen internal combustion engines is the best when the nozzle diameter is 5mm and the hydrogen injection pressure is 3bar.

Keywords: IQGA; Air Intake Blockage; Hydrogen Injection Mass Flow Rate

DOI: 10.57237/j.jest.2023.03.002

1 Introduction

Hydrogen fuel has advantages over traditional gasoline fuel, such as wide ignition limit, fast combustion speed, and less harmful emissions [1, 2]. Moreover, hydrogen fueled internal combustion engines can be retrofitted on the basis of traditional internal combustion engines, so they also have the advantages of low cost and simple retrofitting [3, 4].

In recent years, hydrogen internal combustion engines have been extensively studied by researchers from various countries due to their unique advantages and potential value, leading to continuous improvement in the performance and emissions of hydrogen internal combustion engines. Similar to gasoline engines, hydrogen internal combustion engines also have two injection methods for fuel, namely Port Fuel Injection (PFI) and Hydrogen Direct Injection (HDI) [5, 6]. Among

*Corresponding author: Ping Guo, 486855592@qq.com

Received: April 13, 2023; Accepted: June 15, 2023; Published Online: June 29, 2023 http://www.energyscitech.org

them, HDI technology has relatively higher requirements for nozzle pressure, sealing, corrosion prevention, and durability, and the control strategy is more complex. If a suitable injection strategy cannot be found, it will prevent the complete combustion of hydrogen gas and increase the unburned hydrogen gas during the exhaust process by six times, accompanied by a decrease in thermal efficiency [7, 8]. In contrast, PFI hydrogen internal combustion engines can better adjust parameters such as hydrogen injection pressure, hydrogen injection timing, and nozzle structure, thereby improving the quality of H2/Air mixture, achieving the goal of increasing power and reducing NOx emissions [9-11]. However, when using intake duct injection, high-pressure hydrogen gas rapidly expands after entering the intake duct through the nozzle, reducing the effective flow area and hindering the fresh charge from entering the cylinder [12, 13], resulting in problems such as intake blockage [14].

Roman Button et al. [15] found that the larger the hydrogen injection mass flow rate, the more severe the inlet blockage caused by the expansion of the hydrogen jet. The mass flow rate of hydrogen injection is determined by both the nozzle diameter and the hydrogen injection pressure. Reducing the nozzle diameter and the hydrogen injection pressure alone can reduce the intake blockage caused by hydrogen expansion [16-18]. In order to solve the problem of intake blockage in hydrogen internal combustion engines, this article uses quantum genetic algorithm and improved quantum genetic algorithm to optimize the nozzle diameter and hydrogen injection pressure, find the optimal nozzle diameter and hydrogen injection pressure, and then solve the problem of intake blockage.

Quantum Genetic Algorithm (QGA) is a new probabilistic evolutionary algorithm that combines genetic algorithm and quantum computing [19]. Among them, quantum computing is an emerging interdisciplinary science in the fields of information science and quantum science. In 1996, Narayanan and Moore first proposed the quantum genetic algorithm and successfully applied it to solve the TSP problem [20]. The first quantum algorithm used for factorization was proposed by Shor [21]. In addition, Grover [22] also proposed a quantum algorithm for database random search, reducing the complexity of the algorithm.

Zakaria Laboudi and Salim Chikhi [23] compared quantum genetic algorithm (QGA) with traditional genetic algorithm (CGA) and outlined the computational methods of QGA. The research results indicate that quantum genetic algorithm can maintain efficiency and performance while exploring large search spaces, making it a very promising computing tool. Huaixiao Wang, Jianyong Liu et al. [24] studied the improvement of quantum genetic algorithm and its application in function optimization. In order to accelerate the evolution process and improve the efficiency and accuracy of finding the optimal solution of the algorithm, researchers have proposed several methods to improve traditional quantum genetic algorithms: adaptive rotation angle strategy, quantum crossover operation, quantum mutation operation, and quantum catastrophe operation. The research results show that compared with traditional quantum genetic algorithms, the improved quantum genetic algorithm has increased the probability of finding the optimal solution, faster convergence speed, higher convergence accuracy, and greatly improves the efficiency of traditional quantum genetic algorithms.

Researchers have proposed a new quantum genetic algorithm, QGA3, based on quantum division and its applications. Compared with traditional two-level quantum systems, quantum genetic algorithms based on three-level quantum systems not only accelerate the evolution process, but also are more accurate and effective. [25] Anrong Xue, Wanlin Yang et al. [26] applied a combination of quantum genetic algorithm, particle filter (PF), and generalized regression neural network (GRNN) to estimate the health status of lithium-ion batteries, which is of great significance for estimating the SOH of electric vehicle batteries under actual operating conditions.

At present, research on alleviating intake blockage in PFI hydrogen internal combustion engines is mostly limited to alleviating intake blockage from the perspective of turbocharging, with very few studies addressing intake blockage from the perspectives of hydrogen injection methods and hydrogen injection mass flow rate [27]. Based on this, this article takes a Jialing JH-600 single cylinder hydrogen internal combustion engine as the foundation, and studies how to alleviate intake blockage at medium and low speeds from two aspects: hydrogen injection method and hydrogen injection mass flow rate, thereby further improving the comprehensive performance of the hydrogen internal combustion engine. The main research focuses on the critical hydrogen injection mass flow rate of PFI hydrogen internal combustion engines without backflow, which alleviates intake blockage, as well as the effects of different nozzle

diameters and hydrogen injection pressure on improving the performance of hydrogen internal combustion engines.

2 Models and Research Methods

2.1 Geometric Modeling

The research object is a four valve intake port injection hydrogen internal combustion engine modified from a Jialing JH600 single cylinder four stroke internal combustion engine. Some of its institutional parameters are shown in Table 1:

Table 1 Engine specifications

Parameter	numerical value
Bore/mm	94
Stroke/mm	85
Compress ratio	9.7
Maximum power/kW	30 (6000r/min)
Maximum torque/(N.m)	51 (4500r/min)

The 3D modeling software used is ProE, and the simulation software is AVL-FIRE developed by AVL Company in Austria. While ensuring calculation accuracy, it is necessary to ensure reasonable calculation time. After grid independence verification, the optimal number of grids for different cycles was obtained. The crankshaft angle and mesh quantity corresponding to the working cycle of the model grid are shown in Table 2:

Table 2 Work Cycle

name	crankshaft angle	Number of grids
Valve overlap	351~394 ℃A	450 thousand
air admission	394~634 ℃A	330 thousand
Compression work	634~866 ℃A	200 thousand
exhaust	866~1071 ℃A	300 thousand
TDC	360 ℃A	-
BDC	540 ℃A	-

2.2 Numerical Model

The simulation software AVL FIRE used in this study is a three-dimensional numerical simulation, which is the focus of the study. The selection criteria for various numerical models are not detailed here, and only some numerical calculation model selections are shown in Table 3:

Table 3 Calculation Model

	Model
turbulence model	k-ζ-f
Combustion model	ECFM-3Z
Emission model	Zeldovich

2.3 Research Protocol Setting

Figure 1 shows the variation curve of air inlet mass flow rate with crankshaft angle for PFI hydrogen internal combustion engines at different speeds:

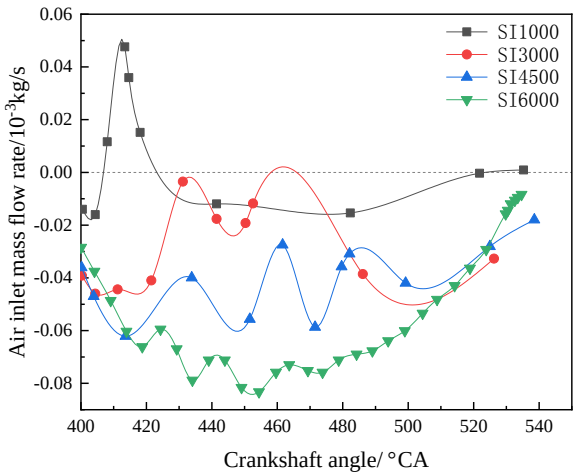

Figure 1 The trend of air inlet mass flow rate changing with crankshaft angle at different rotational speeds

When the mass flow rate at the air inlet is below the 0 mark, it indicates that the direction of air movement is along the direction of the inlet; When the mass flow rate at the air inlet is higher than the 0 mark, it indicates that air is flowing back from the intake duct to the gas collection box, indicating that the intake blockage has occurred at this time. From Figure 1, it can be seen that the flow rate in the engine inlet increases with the increase of engine speed, and when the speed is above 3000r/min, there will be no intake backflow phenomenon. Therefore, this article mainly selects the minimum stable speed of the engine of 1000r/min as the representative speed to study the intake blockage at low speeds, and selects a working condition with an excess air coefficient of 1.5, i.e. an equivalent ratio of 0.67, for research. In order to achieve different hydrogen injection flows, this section combines different nozzle diameters and hydrogen injection pressures. Among them, the nozzle diameter is selected as 3, 3.5, 4, 4.5, and 5mm, and the injection pressure is selected as 1.5 bar, 2 bar, 2.5 bar, 3 bar, 3.5 bar, and 4 bar. The combination of the two parameters can achieve various hydrogen injection flows, thus achieving various working conditions. Table 4 shows the specific research protocol:

Table 4 Research Plan

parameter	horizontal					
Orifice diameter/mm	3	3.5	4	4.5	5	
Hydrogen injection pressure/bar	1.5	2	2.5	3	3.5	4

2.4 Model Validation

To ensure the reliability of simulation test simulation, experimental data and simulation simulation data were compared for a working condition of 1000r/min and an equivalence ratio of 0.67. As shown in Figure 2, the simulation values were slightly higher than the experimental values. The main reason is that the simulated working conditions are ideal, assuming that the cylinder is fully enclosed, but there may be some errors in actual experiments, with a maximum difference of 1.2%, It is believed that this model can well reflect the working conditions of hydrogen engines in practice.

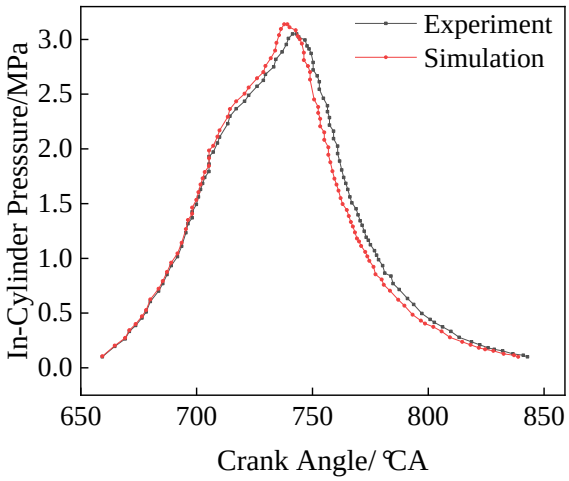

Figure 2 Model Validation

2.5 Quantum Genetic Algorithm

Quantum genetic algorithm (QGA) is a kind of genetic algorithm based on the principle of quantum computing. This algorithm is based on the state vector representation of quantum. It applies the probability amplitude representation of quantum bits to the coding of chromosomes, so that a chromosome can express the superposition of multiple states, and uses quantum logic gates to realize the update operation of chromosomes, achieving better results than conventional genetic algorithms, Furthermore, the optimization solution of the goal was achieved [28]. The traditional quantum genetic algorithm [29] has some shortcomings: premature convergence leads to premature loss of population diversity, and the optimal solution obtained is often a local optimal solution; Insufficient local search performance results in the latter having a slower convergence speed and being unable to converge to the global optimal solution during the evolution stage.

Compared with QGA, the improved quantum genetic algorithm (IQGA) can dynamically adjust the rotation angle of quantum gate according to the evolution process. In the initial stage of the algorithm, a larger rotation angle is set, and gradually decreases with the increase of evolutionary algebra. The adjustment strategy is to measure the individual, evaluate its fitness, compare it with the fitness value f (best) of the retained optimal individual, and adjust the corresponding bit quantum bits according to the comparison results, so as to make it evolve in the direction conducive to the optimal determination of the solution. In addition, IQGA also incorporates quantum mutation operations and quantum catastrophe operations. Improved the structure of traditional quantum algorithms and improved the evolutionary efficiency of traditional quantum genetic algorithms [30].

Among them, $Q(t_0)$ is the initialization population, which includes all genes of all chromosomes in the population (α_i^t, β_i^t) all are initialized as $(\frac{1}{\sqrt{2}}, \frac{1}{\sqrt{2}})$, this means that a chromosome expresses an equal probability superposition of all its possible states:

$$\left|\Psi_{q_j}^t\right\rangle = \sum_{k=1}^{2^m} \frac{1}{\sqrt{2^m}} |S_k\rangle \quad (1)$$

Measure all individuals in Q (t) and obtain a set of solutions p(t). $p(t)=\left\{p_1^t, p_2^t, \cdots, p_n^t\right\}$, Is the jth ($j = 1, 2, \ldots, n$). The entire measurement process is as follows: randomly generate [0,1] numbers, and reduce the probability of quantum bits $\left|\alpha_i^t\right|^2$or $\left|\beta_i^t\right|^2$(i=1，2，…，n)compare with the generated number, If the number is greater than $\left|\alpha_i^t\right|^2$ or $\left|\beta_i^t\right|^2$, the result obtained is 1, otherwise it is 0. Then, evaluate the fitness of this group of solutions, and record the best fitness individual as the target value for the next evolution.

Subsequently, the algorithm enters a cyclic iteration stage, and as the iteration progresses, the solution of the population gradually converges towards the optimal solution. In each iteration, the population is first measured to obtain a set of deterministic solutions P (t), Then calculate the fitness value of each solution, and use the quantum rotary gate to adjust the individuals in the population according to the current evolution goal and the predetermined adjustment strategy to obtain the updated population, record the current optimal solution, and compare it with the current target value. If it is greater

than the current target value, the new optimal solution will be used as the target value of the next iteration, otherwise the current target value will remain unchanged.

The flowchart of quantum genetic algorithm is shown in Figure 3.

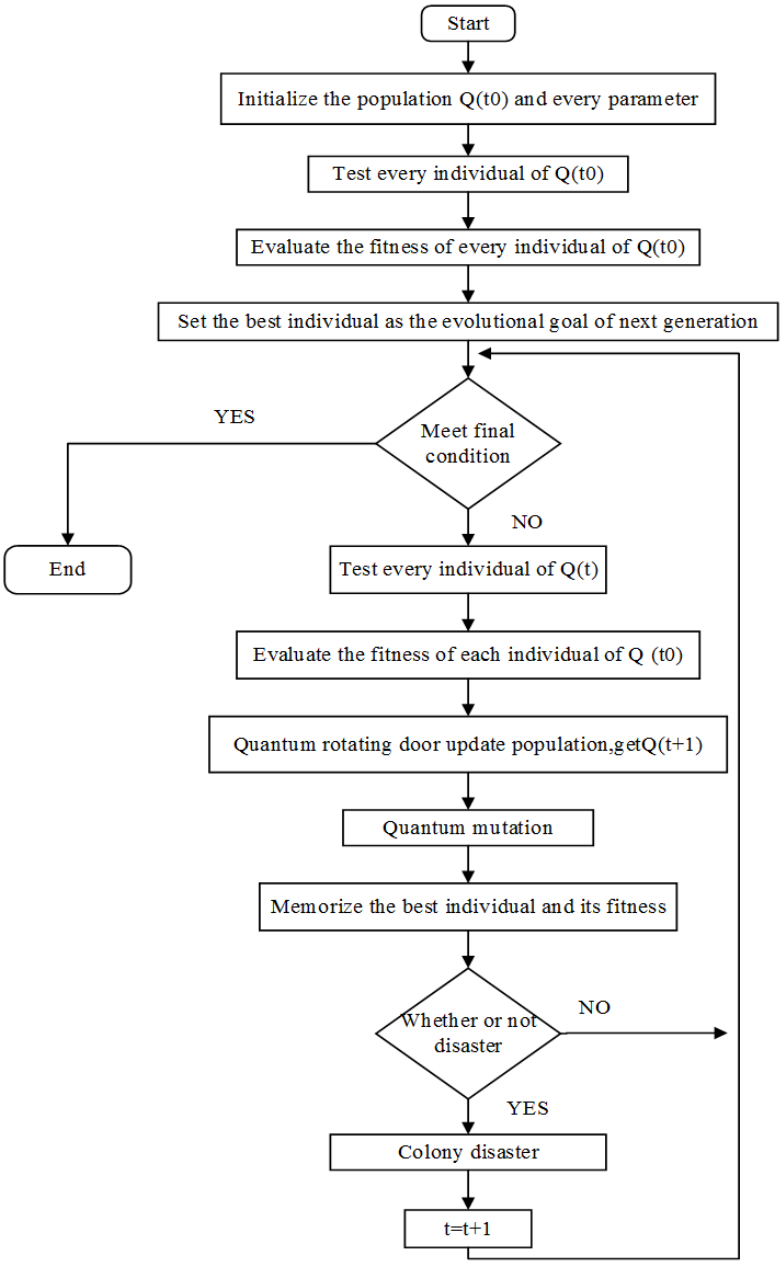

Figure 3 IQGA Flow Chart

3 The Effect of Hydrogen Injection Flow Rate on Hydrogen Internal Combustion Engines

The greater the flow rate of hydrogen injection, the more severe the inlet blockage caused by the expansion of the hydrogen jet [31]. The hydrogen mass flow rate is determined by both the nozzle diameter and the hydrogen injection pressure. Therefore, the influence of hydrogen mass flow rate on inlet blockage is studied from the perspectives of nozzle diameter and hydrogen injection pressure.

3.1 Impact on Alleviating Intake Blockage in Hydrogen Internal Combustion Engines

At the same initial moment of hydrogen injection, but with different nozzle diameters and hydrogen injection pressures, in order to achieve the same equivalence ratio, it is necessary to control the end time of hydrogen injection [32]. The hydrogen injection starts at 404 ℃A, and the end of hydrogen injection under different operating conditions is known to be before the piston reaches the top dead center. Table 5 shows the end angles of hydrogen injection under different nozzle diameters and hydrogen injection pressures.

Table 5 End angle of hydrogen injection(℃A)

	1.5bar	**2bar**	**2.5bar**	**3bar**
3mm	485	461.5	443.8	442
4mm	453.75	438.5	431.5	429.5
5mm	429	422.5	417	414.5

Under different nozzle diameters and hydrogen injection pressures, the mass flow rate of hydrogen injection holes fluctuates differently. Figure 4 shows the variation trend of mass flow rate of hydrogen injection holes with crankshaft angle under different nozzle diameters and hydrogen injection pressures.

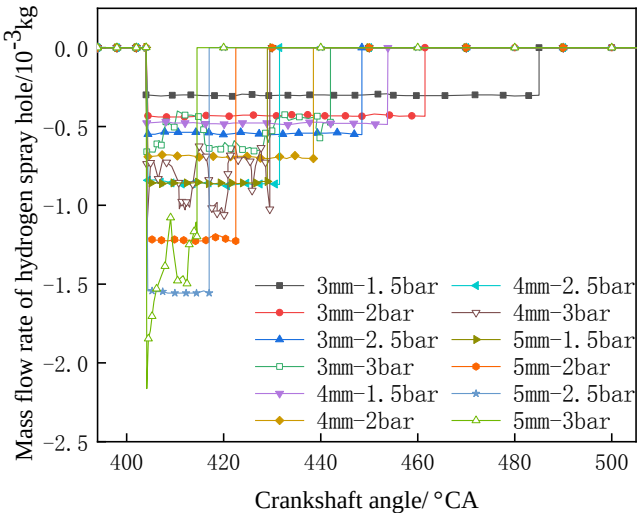

Figure 4 Mass flow rate of hydrogen nozzle

From Figure 4, it can be observed that during the duration of hydrogen injection, the flow rate of hydrogen injection pore material is not relatively stable under all operating conditions. Through comparison, it can be found that the main factor determining the stability of hydrogen injection pore material flow rate is the hydrogen injection pressure. When the hydrogen injection pressure is not higher than 2.5 bar, regardless of the diameter of the nozzle, the flow rate of hydrogen injection pore material is at a relatively stable value. However, when the hydrogen injection pressure is 3 bar, the flow rate of hydrogen injection pore material fluctuates violently, The higher the hydrogen injection pressure, the greater the frequency and amplitude of the change in the mass flow rate of the hydrogen injection pore. In theory, the greater the pressure, the greater the hydrogen injection flow rate [33]. However, this is not the case. When the pressure exceeds 3 bar, the hydrogen injection flow rate will fluctuate violently, leading to a decrease in the average hydrogen injection flow rate. Table 6 shows the average hydrogen injection flow rate at the nozzle under different working conditions.

Table 6 Average Hydrogen Injection Mass Flow Rate (10^{-3}kg/s)

	1.5bar	**2bar**	**2.5bar**	**3bar**
3mm	0.30	0.43	0.54	0.53
4mm	0.48	0.69	0.85	0.81
5mm	0.86	1.21	1.53	1.41

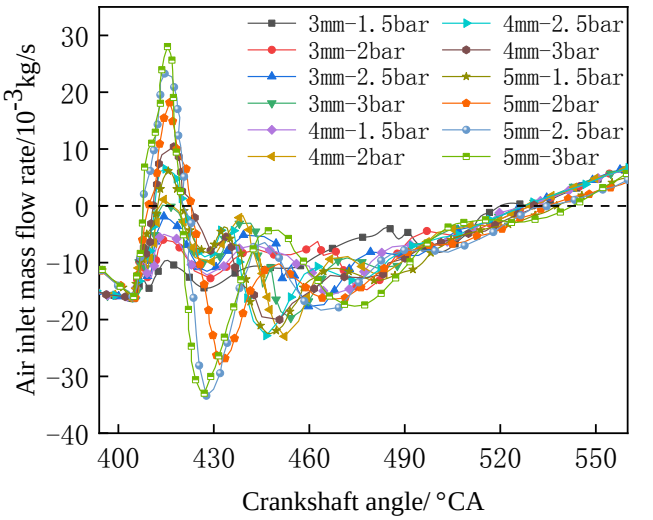

Figure 5 Change of air inlet mass flow rate with crankshaft angle

Figure 5 shows the variation of air inlet mass flow rate with crankshaft angle under different hydrogen injection flow conditions. After the injection of hydrogen from 404 ℃A, there was a short-term sharp decrease in the instantaneous mass flow rate at the air inlet under all twelve operating conditions. The slope of the decrease was not significantly different when the nozzle diameter was 3mm and 4mm, with a 5mm decrease slope slightly higher than the other two nozzle diameters. The main

reason is that the pressure at the hydrogen nozzle suddenly increases, causing a pressure wave to be generated in the inlet, which propagates inside the inlet. After a sharp decline, there was a brief rebound, followed by a sharp decline again. However, at this point, it can be seen that as the hydrogen injection mass flow rate increases, the slope of rise and fall also increases. This is because the diffusion coefficient of hydrogen gas is high, and high-pressure hydrogen gas will rapidly expand after being injected into the inlet duct, occupying a portion of the inlet space, reducing the effective cross-sectional area of fresh air circulation. By carefully comparing various experimental conditions, it can be found that as the hydrogen injection flow rate increases, the duration of the sharp decrease also increases. This indicates that the larger the hydrogen injection flow rate, the more severe the "blockage" of the inlet duct, and the greater the impact on the air flow rate. Although the injection of high-pressure hydrogen gas reduces the effective cross-sectional area of fresh air flow, it can be seen from Figure 4 that under all operating conditions, the fresh air flow rate did not fluctuate around a fixed value after a sharp decrease during the hydrogen injection period. Instead, after a sharp decrease, a rapid rebound process occurred again, and all reached a certain peak around 440 ℃A. The reason for this phenomenon is that the volumetric flow rate in the engine intake duct reaches its maximum value at around 430 ℃A under reverse drag conditions, while under hydrogen injection conditions, the mixture density in the intake duct decreases, the inertia decreases, and the peak volumetric flow rate is delayed. At the same time, the rapid expansion of hydrogen gas previously caused a decrease in fresh air volumetric flow rate, but the sum of hydrogen volumetric flow rate and the reduced air volumetric flow rate is less than the peak volumetric flow rate after the delay mentioned above. In deeper comparison, it was found that when the inlet gas flow rate was higher than 2.29kg/h, there was a phenomenon of air flowing out of the air inlet cross-section in the middle stage of intake. With the increase of hydrogen injection mass flow rate, the instantaneous mass flow rate during fresh air backflow increased and the duration became longer. This indicates that under low-speed operating conditions, if an excessive hydrogen injection flow rate is used, it will cause a backflow phenomenon of fresh air in the middle of the intake air. The larger the flow rate, the greater the instantaneous flow rate of the back flow, and the longer the duration.

3.2 Configuration Strategy Based on Quantum Genetic Algorithm

Using the improved quantum genetic algorithm (IQGA) to optimize the nozzle diameter and hydrogen injection pressure, find the optimal nozzle diameter and hydrogen injection pressure, and achieve the goal of alleviating intake blockage in hydrogen internal combustion engines. In order to verify the optimization effect of the improved quantum genetic algorithm, traditional quantum genetic algorithm optimization was used as the control group, with 200 iterations and 5 runs of each algorithm for optimization, as shown in Figure 8. The comprehensive objective function is:

$$min\ Y = -(15.35 - 30.34x_1 + 12.69x_2 + 4.15x_1^2 - 3.92x_2^2 + 3.9x_1x_2) \quad (2)$$

In the formula, Y represents the maximum return flow rate; X1 is the diameter of the spray hole; X2 is the hydrogen injection pressure.

(1) Quantum bit encoding. The genes encoding m parameters using multiple qubits are as follows:

$$q_j^t = \begin{pmatrix} \alpha_{11}^t & \alpha_{12}^t & \cdots & \alpha_{1k}^t & \alpha_{21}^t & \alpha_{22}^t & \cdots & \alpha_{2k}^t & \alpha_{m1}^t & \alpha_{m2}^t & \cdots & \alpha_{mk}^t \\ \beta_{11}^t & \beta_{12}^t & & \beta_{1k}^t & \beta_{21}^t & \beta_{22}^t & & \beta_{2k}^t & \beta_{m1}^t & \beta_{m2}^t & & \beta_{mk}^t \end{pmatrix} \quad (3)$$

Among them, represents the chromosome of the i-th generation and jth individual; K is the number of quantum bits encoding each gene; M is the number of genes on a chromosome.

Initialize the quantum bit encoding of each individual in the population to, which means that all possible states expressed by a chromosome are equally probable.

(2) Adjustment operation of quantum revolving door:

$$U(\theta_i) = \begin{bmatrix} cos(\theta_i) & -sin(\theta_i) \\ sin(\theta_i) & cos(\theta_i) \end{bmatrix} \begin{bmatrix} \alpha_i \\ \beta_i \end{bmatrix} \quad (4)$$

The update process is as follows:

$$\begin{bmatrix} \alpha_i' \\ \beta_i' \end{bmatrix} = U(\theta_i) \begin{bmatrix} \alpha_i \\ \beta_i \end{bmatrix} = \begin{bmatrix} cos(\theta_i) & -sin(\theta_i) \\ sin(\theta_i) & cos(\theta_i) \end{bmatrix} \begin{bmatrix} \alpha_i \\ \beta_i \end{bmatrix} \quad (5)$$

Where, $(\alpha_i, \beta_i)^T$ and $(\alpha_i', \beta_i')^T$ represent the probability amplitude θ_i before and after the update of the ith quantum bit revolving door of chromosome, which is the rotation angle, and its size and symbol are determined by the preset adjustment strategy.

From the formula, it can be concluded that$\alpha_i'$and β_i' are respectively

$$\begin{cases} \alpha_i^t = \alpha_i cos(\theta_i) - \beta_i sin(\theta_i) \\ \beta_i^t = \alpha_i sin(\theta_i) + \beta_i cos(\theta_i) \end{cases} \quad (6)$$

Therefore

$$|\alpha_i'|^2 + |\beta_i'|^2 = [\alpha_i cos(\theta_i) - \beta_i sin(\theta_i)]^2 + [\alpha_i sin(\theta_i) + \beta_i cos(\theta_i)]^2 = |\alpha_i|^2 + |\beta_i|^2 = 1 \quad (7)$$

We can see that the value of $|\alpha_i'|^2 + |\beta_i'|^2$ after the transformation is still 1.

Among them, x_i is the i-th position of the current chromosome; $best_i$ is the i-th position of the current optimal chromosome; f(x) is the fitness function; $s(\alpha_i, \beta_i)$ is the direction of rotation angle; $\Delta\theta_i$ is the size of the rotation angle, and its value is determined based on the selection strategy listed in the table. The adjustment strategy is to compare the fitness f(x) of the current measured value of individual q_j^t with the fitness $f(best_i)$ of the current optimal individual of the population. If $f(x)>f(best_i)$, adjust the corresponding quantum bits in q_j^t, so that the probability amplitude evolves in favor of the emergence of x_i for (α_i, β_i); On the contrary, if $f(x)<f(best_i)$, adjust the corresponding bits of q_j^t in order to make the probability amplitude of (α_i, β_i) evolve in a direction that is favorable for the occurrence of best.

The rotation angle selection strategy is shown in Figure 7:

Table 7 Rotation angle

x_i	$best_i$	f(x) > f(best)	$\Delta\theta_i$	$s(\alpha_i, \beta_i)$			
				$\alpha_i\beta_i>0$	$\alpha_i\beta_i<0$	$\alpha_i=0$	$\beta_i=0$
0	0	FALSE	0	0	0	0	0
0	0	TRUE	0	0	0	0	0
0	1	FALSE	0.01π	+1	-1	0	±1
0	1	TRUE	0.01π	-1	+1	±1	0
1	0	FALSE	0.01π	-1	+1	±1	0
1	0	TRUE	0.01π	+1	-1	0	±1
1	1	FALSE	0	0	0	0	0
1	1	TRUE	0	0	0	0	0

From Figure 7, it can be seen that QGA converges near the optimal solution around 50 generations, but is very unstable. It tends to stabilize at 100 generations, but there are still small fluctuations, indicating that despite convergence, the optimal solution may still change. IQGA reached its optimal solution during approximately 20 generations of operation, and the optimization results were the same during 50 generations of operation. Therefore, compared to QGA, IQGA has faster convergence speed and good stability. This is because IQGA adds quantum mutation operation and quantum catastrophe operation than QGA, and its pseudocode is shown in Figure 6. Quantum mutation operation helps to increase population diversity and reduce the probability of premature convergence; Quantum catastrophe operation can obtain stable local optimal solutions, and this operation can interfere with certain individuals in the population, regenerating some new random individuals.

According to the optimization results of QGA and IQGA, it is known that the maximum return flow rate is the smallest when the nozzle diameter is 3mm and the hydrogen injection pressure is 1.5bar, which can alleviate the problem of intake blockage in hydrogen internal combustion engines.

The evolution process obtained by optimizing 200 generations of QGA and IQGA is shown in Figure 7.

```
Procedure Mutate (p_i)
Begin
  If p_i is not the current optimum chromosome then
  Begin
    j = 0;
    When (j < n)
    j = j + 1;
    Generate Random Number rand in range (0, 1);
    If rand < α or rand < β
    Exchange α and β;
  End
End

Begin
  If (disaster-condition)
  Begin
  If (The chromosome is not the best chromosome)
  Initialize the chromosome;
  End
End
```

Figure 6 Pseudocode

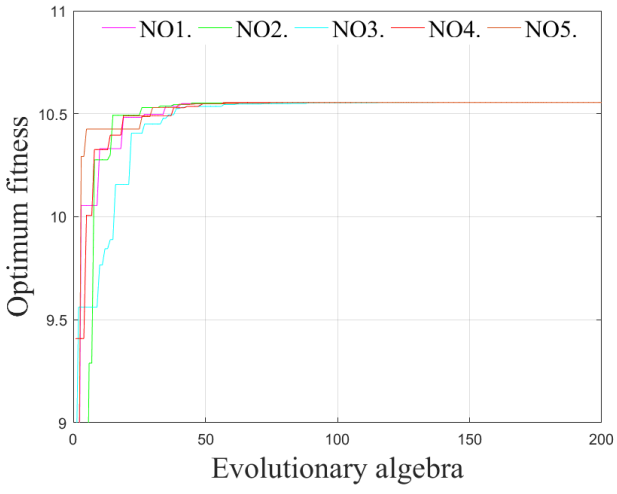

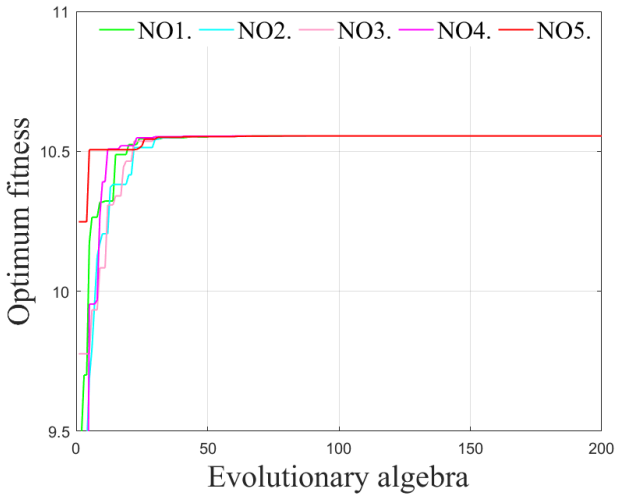

Figure 7 Algorithm Optimization

3.3 Comprehensive Performance Evaluation Indicators

3.3.1 Impact on the Economy and Power Performance of Hydrogen Internal Combustion Engines

The hydrogen internal combustion engine needs to improve its thermal efficiency and output power as much as possible while eliminating intake blockage. The impact trend of nozzle diameter and hydrogen injection pressure on the economy and power of the hydrogen internal combustion engine is different from the impact trend on intake blockage. Figures 8 and 9 show the variation trend of indicated power and indicated thermal efficiency of the hydrogen engine with nozzle diameter and hydrogen injection pressure. As shown in the figure, with the increase of nozzle diameter and hydrogen injection pressure, the indicated thermal efficiency and indicated power of hydrogen internal combustion engines show a trend of first increasing and then decreasing, and both reach their maximum values when the nozzle diameter is 3.5mm; As the hydrogen injection pressure increases, the indicated thermal efficiency and indicated power of the hydrogen internal combustion engine also show a trend of first increasing and then decreasing. When the hydrogen injection pressure is 3 bar, the indicated thermal efficiency and indicated power reach their maximum values.

In the research results of the previous chapter, it was found that when the pressure exceeds 3 bar, the hydrogen injection flow rate will undergo drastic fluctuations, leading to a decrease in the average hydrogen injection flow rate. When the hydrogen injection pressure is below 3 bar, the indicated thermal efficiency and power increase with the increase of hydrogen injection pressure. When the hydrogen injection pressure is higher than 3 bar, the indicated thermal efficiency and indicated power decrease with the increase of hydrogen injection pressure. From this, it can be concluded that the power and economy of hydrogen engines are mainly affected by the injection pressure of hydrogen. When the injection pressure is 3 bar, it reaches strong power and excellent economy.

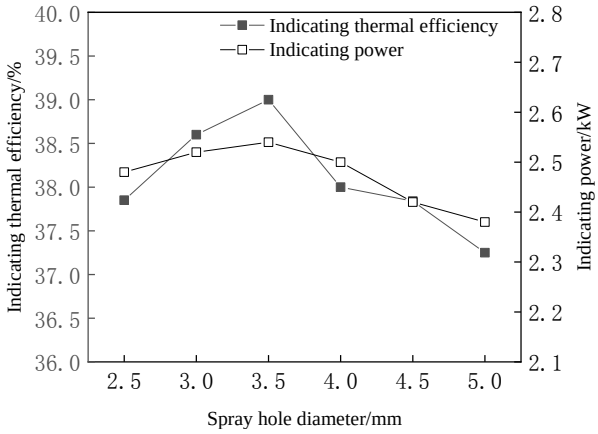

Figure 8 Trend of indicated thermal efficiency and indicated power with nozzle diameter

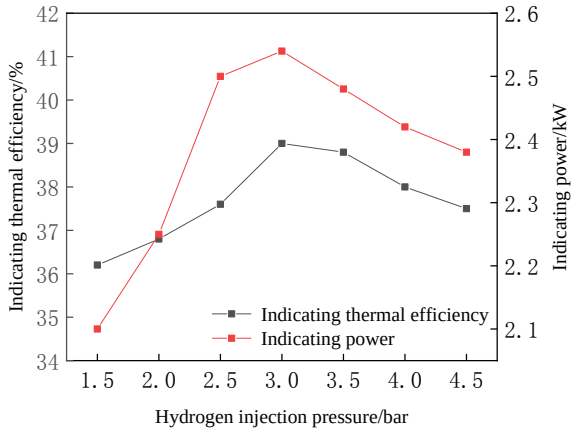

Figure 9 Trend of indicated thermal efficiency and indicated power with hydrogen injection pressure

3.3.2 Impact on Emissions from Hydrogen Internal Combustion Engines

Figures 10 and 11 show the variation curves of NO generation mass fraction with nozzle diameter and hydrogen injection pressure, respectively. As shown in Figure 10, as the diameter of the nozzle increases, the

amount of NO generation first increases and then sharply decreases, and a peak appears at a diameter of 4mm. This is because as the diameter of the nozzle increases, the maximum pressure and maximum combustion temperature in the cylinder gradually increase. The high temperature at a nozzle diameter of 4mm is conducive to the generation of NO, leading to the peak emission of NO; After the nozzle diameter is greater than 4mm, the maximum pressure and maximum combustion temperature in the cylinder rapidly decrease, resulting in a sharp decrease in NO generation.

As shown in Figure 11, the NO mass fraction shows a trend of first increasing and then decreasing with the increase of hydrogen injection pressure, and reaches its peak at 3.5 bar. Because at a hydrogen injection pressure of 3.5 bar, the uniformity of the cylinder mixture, combustion rate, and average temperature in the cylinder are better than other times, further promoting the generation of NO.

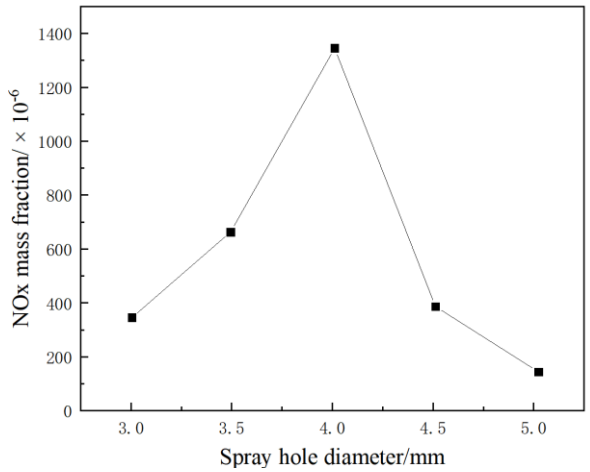

Figure 10 NOx mass fraction under different nozzle diameters

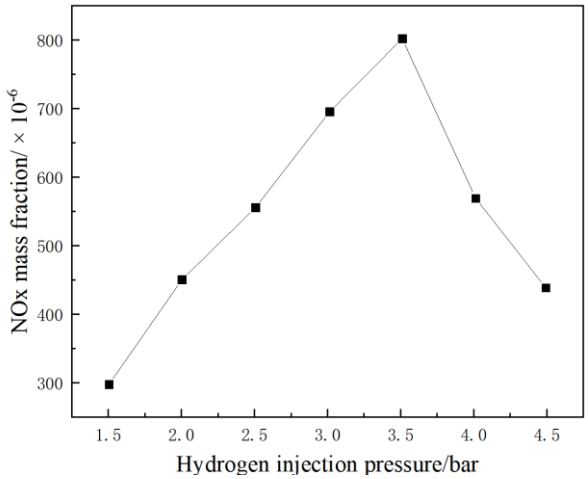

Figure 11 NOx mass fraction under different hydrogen injection pressures

3.3.3 Comprehensive Evaluation

Adopting different nozzle diameters and hydrogen injection pressure can improve power performance while also causing changes in economy and emissions. Therefore, the comprehensive performance of hydrogen internal combustion engines cannot be evaluated using a single indicator, but rather through dimensionless and weighted methods.

(1) The values of different evaluation indicators are not in the same order of magnitude and need to be uniformly dimensionless. Choose the following formula to perform dimensionless processing on the data.

$$y_i = \frac{x_i}{x_{max}} \times 100 \tag{8}$$

In equation (8), y_i is the evaluation index value after dimensionless transformation, x_i is the evaluation index value before dimensionless transformation, and x_{max} is the maximum value among the evaluation indexes before dimensionless transformation.

(2) Determining the combination weight of indicators based on game theory

Game theory mainly studies the interaction between formulaic incentive structures, and is a mathematical theory and method for studying phenomena with the nature of struggle or competition. This article uses a combination weighting method composed of Analytic Hierarchy Process (AHP) and Entropy Weighting to weight various evaluation indicators [34]. Among them, AHP belongs to the subjective weighting method and has a strong subjectivity in weight allocation; The entropy weighting method is a completely based method for assigning weights to experimental data. When the number of experimental data groups is small, abnormal data may occur. Therefore, combining subjective evaluation makes weight allocation more reasonable.

The different weights obtained by the analytic hierarchy process (AHP) and entropy weighting method are solved by the method of game theory to find the equilibrium solution, and the final weight distribution is obtained.

The subjective weight W1 determined by the AHP method is (w_{11}, w_{12}, w_{13}), while the objective weight W_2 determined by the entropy method is (w_{21}, w_{22}, w_{23}).

The optimal combination weight of evaluation indicators is

$$W^* = 0.714W_1 + 0.286W_2 \tag{9}$$

The weights of various evaluation indicators obtained from the above equation are shown in Table 8.

Table 8 Weights of various evaluation indicators

Index weight	Economy	Dynamicity	Emissions
Subjective weight	0.40	0.40	0.20
Objective weight	0.47	0.26	0.27
Combination weight	0.42	0.36	0.22

(3) From previous research, it can be seen that when the hydrogen injection pressure is 3 bar, the indicated thermal efficiency and indicated power of the hydrogen internal combustion engine reach their peak. Therefore, fix the hydrogen injection pressure at 3 bar and study the comprehensive performance of hydrogen internal combustion engines with different nozzle diameters at 3 bar.

(4) The final comprehensive evaluation index is obtained by weighting the dimensionless data according to the weights obtained by the combination weighting method, as shown in Table 9:

Table 9 Comprehensive Evaluation Index Values

Aperture diameter	Economy	Dynamicity	Emissions	Synthesize
3	42	36	19.95	58.05
3.5	42	36	20.40	57.60
4	42	36	20.91	57.09
4.5	42	36	20.03	57.97
5	42	36	19.52	58.48

From the comprehensive evaluation index values shown in Figure 12, it can be seen that the hydrogen internal combustion engine has the best comprehensive performance under the working condition of a nozzle diameter of 5 when the hydrogen injection pressure is fixed at 3 bar.

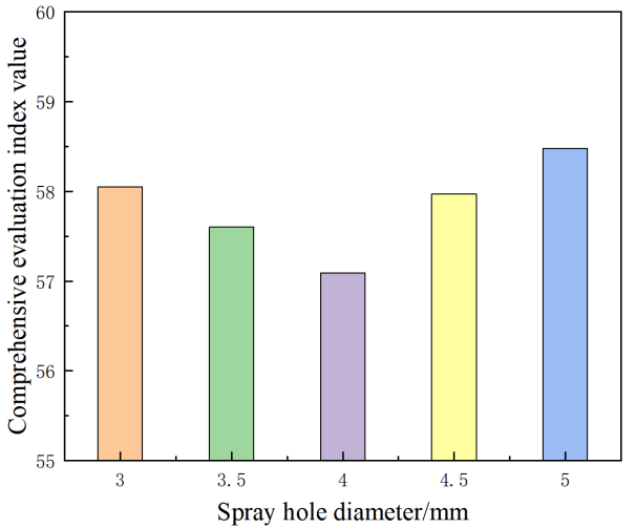

Figure 12 Comprehensive performance evaluation index values of hydrogen internal combustion engines with different nozzle diameters

4 Conclusion

In this study, the combination of IQGA and combined weighting method was used to optimize the nozzle diameter and hydrogen injection pressure of a hydrogen engine. The specific conclusions are as follows:

(1) As the diameter of the hydrogen injection hole increases, the mass flow rate of the hydrogen injection increases, and the degree of inlet blockage worsens; As the hydrogen injection pressure increases, the mass flow rate first increases and then decreases. When the hydrogen injection pressure is 3 bar, there is a change and the degree of inlet blockage worsens. The diameter of the nozzle has a greater impact on inlet blockage than the pressure of hydrogen injection. The flow rate of hydrogen injection is the final factor determining inlet blockage, and there is a strict linear relationship between the maximum return flow rate and the flow rate of hydrogen injection;

(2) According to the optimization results of QGA and IQGA, it is known that the maximum return flow rate is the smallest when the nozzle diameter is 3mm and the hydrogen injection pressure is 1.5bar, which can alleviate the problem of inlet blockage in hydrogen internal combustion engines;

(3) From the comprehensive evaluation index values, it can be seen that the hydrogen internal combustion engine has the best comprehensive performance under the working condition of a nozzle diameter of 5 when the hydrogen injection pressure is fixed at 3 bar.

This article uses quantum genetic algorithm to optimize the nozzle diameter and hydrogen injection flow rate, aiming to find the optimal nozzle diameter and hydrogen injection pressure under different operating conditions, and then find the optimal hydrogen injection flow rate to significantly improve the comprehensive performance of hydrogen internal combustion engines. However, due to workload limitations, this article still has certain shortcomings and shortcomings. In the future, we need to search for more parameters for optimization and study together with other operating parameters to ultimately achieve the goal of improving the performance of hydrogen internal combustion engines.

References

[1] Dang J, Wang L. Optimization control of hydrogen engine ignition system based on ACO-BP [J]. International journal of hydrogen energy, 2021 (78): 46.

[2] Wei H, Zhang R, Chen L, et al. Effects of high ignition energy on lean combustion characteristics of natural gas using an optical engine with a high compression ratio [J]. Energy, 2021, 223: 120053.

[3] Shi C, Chai S, Di L, et al. Combined experimental-numerical analysis of hydrogen as a combustion enhancer applied to wankel engine [J]. Energy, 2022: 125896.

[4] Anupong W, On-uma R, Jutamas K, et al. Utilization of enriched hydrogen blends in the diesel engine with MgO nanoparticles for effective engine performance and emission control [J]. Fuel, 2023, 334: 126552.

[5] Liu X, Srna A, Yip H L, et al. Performance and emissions of hydrogen-diesel dual direct injection (H2DDI) in a single-cylinder compression-ignition engine [J]. International Journal of Hydrogen Energy, 2021, 46 (1): 1302-1314.

[6] Chen W, Yu S, Zuo Q, et al. Combined Effect of Air Intake Method and Hydrogen Injection Timing on Airflow Movement and Mixture Formation in a hydrogen direct injection rotary engine [J]. International Journal of Hydrogen Energy, 2022, 47 (25): 12739-12758.

[7] Ravi N, Liao H H, Jungkunz A F, et al. Model predictive control of HCCI using variable valve actuation and fuel injection [J]. Control Engineering Practice, 2012, 20 (4): 421-430.

[8] Wei Y, Fan L, Zhang H, et al. Experimental investigations into the effects of string cavitation on diesel nozzle internal flow and near field spray dynamics under different injection control strategies [J]. Fuel, 2022, 309: 122021.

[9] Dinesh M H, Kumar G N. Effects of compression and mixing ratio on NH_3/H_2 fueled Si engine performance, combustion stability, and emission [J]. Energy Conversion and Management: X, 2022, 15: 100269.

[10] Kakoee A, Bakhshan Y, Aval S M, et al. An improvement of a lean burning condition of natural gas/diesel RCCI engine with a pre-chamber by using hydrogen [J]. Energy Conversion and Management, 2018, 166: 489-499.

[11] Xu P, Ji C, Wang S, et al. Effects of direct water injection on engine performance in engine fueled with hydrogen at varied excess air ratios and spark timing [J]. Fuel, 2020, 269: 117209.

[12] Wang L, Yang Z, Huang Y, et al. The effect of hydrogen injection parameters on the quality of hydrogen–air mixture formation for a PFI hydrogen internal combustion engine [J]. International Journal of Hydrogen Energy, 2017, 42 (37): 23832-23845.

[13] Gao W, Fu Z, Li Y, et al. Progress of Performance, Emission, and Technical Measures of Hydrogen Fuel Internal-Combustion Engines [J]. Energies, 2022, 15 (19): 7401.

[14] Ahumada C B, Mannan M S, Wang Q, et al. Hydrogen detonation onset behind two obstructions with unequal blockage ratio and opening geometry [J]. International Journal of Hydrogen Energy, 2022, 47 (73): 31468-31480.

[15] Sato T, Chacon F, Gamba M, et al. Mass flow rate effect on a rotating detonation combustor with an axial air injection [J]. Shock Waves, 2021, 31 (7): 741-751.

[16] Wei S S, Lee M C, Chien Y H, et al. Experimental investigation of the effect of nozzle throat diameter on the performance of a hybrid rocket motor with swirling injection of high-concentration hydrogen peroxide [J]. Acta Astronautica, 2019, 164: 334-344.

[17] Babayev R, Andersson A, Serra Dalmau A, et al. Computational optimization of a hydrogen direct-injection compression-ignition engine for jet mixing dominated nonpremixed combustion [J]. International Journal of Engine Research, 2022, 23 (5): 754-768.

[18] Zhao M, Zhang H. Origin and chaotic propagation of multiple rotating detonation waves in hydrogen/air mixtures [J]. Fuel, 2020, 275: 117986.

[19] Shi F, Wang H, Yu L, et al. Analyze of 30 Cases of MATLAB Intelligent Algorithms [J]. 2010.

[20] Narayanan A, Moore M. Quantum-inspired genetic algorithms [C]//Proceedings of IEEE international conference on evolutionary computation. IEEE, 1996: 61-66.

[21] Shor P W. Algorithms for quantum computation: discrete logarithms and factoring [C]//Proceedings 35th annual symposium on foundations of computer science. Ieee, 1994: 124-134.

[22] Grover L K. A fast quantum mechanical algorithm for database search [C]//Proceedings of the twenty-eighth annual ACM symposium on Theory of computing. 1996: 212-219.

[23] Laboudi Z, Chikhi S. Comparison of genetic algorithm and quantum genetic algorithm [J]. Int. Arab J. Inf. Technol., 2012, 9 (3): 243-249.

[24] Wang H, Liu J, Zhi J, et al. The improvement of quantum genetic algorithm and its application on function optimization [J]. Mathematical problems in engineering, 2013, 2013.

[25] Tkachuk V. Quantum genetic algorithm based on qutrits and its application [J]. Mathematical Problems in Engineering, 2018, 2018: 1-8.

[26] Xue A, Yang W, Yuan X, et al. Estimating state of health of lithium-ion batteries based on generalized regression neural network and quantum genetic algorithm [J]. Applied Soft Computing, 2022, 130: 109688.

[27] Ding H, Zhuo C, Chen X, et al. Numerical study on the transverse jet flow and mixing characteristics of hydrogen/metal powder fuel in powder fuel scramjet [J]. Fuel, 2022, 326: 125088.

[28] Zhu X, Xiong J, Liang Q. Fault diagnosis of rotation machinery based on support vector machine optimized by quantum genetic algorithm [J]. IEEE Access, 2018, 6: 33583-33588.

[29] Cheng G, Wang C, Xu C. A novel hyper-chaotic image encryption scheme based on quantum genetic algorithm and compressive sensing [J]. Multimedia Tools and Applications, 2020, 79 (39-40): 29243-29263.

[30] Zhang J, Qiu X, Li X, et al. Support vector machine weather prediction technology based on the improved quantum optimization algorithm [J]. Computational Intelligence and Neuroscience, 2021, 2021.

[31] Salvadori M, Tudisco P, Ranjan D, et al. Numerical investigation of mass flow rate effects on multiplicity of detonation waves within a H_2/Air rotating detonation combustor [J]. International Journal of Hydrogen Energy, 2022, 47 (6): 4155-4170.

[32] Zambalov S D, Yakovlev I A, Maznoy A S. Effect of multiple fuel injection strategies on mixture formation and combustion in a hydrogen-fueled rotary range extender for battery electric vehicles [J]. Energy Conversion and Management, 2020, 220: 113097.

[33] Tabkhi F, Azzaro-Pantel C, Pibouleau L, et al. A mathematical framework for modelling and evaluating natural gas pipeline networks under hydrogen injection [J]. International journal of hydrogen energy, 2008, 33 (21): 6222-6231.

[34] Sovacool B K, Axsen J, Sorrell S. Promoting novelty, rigor, and style in energy social science: Towards codes of practice for appropriate methods and research design [J]. Energy Research & Social Science, 2018, 45: 12-42.